How to build a loaded thermoacoustic engine

Hiroki Hatori,[1] Tetsushi Biwa,[1] and Taichi Yazaki[2]
[1]*Department of Mechanical Systems and Design, Tohoku University, Sendai, 980–8579 Japan*
[2]*Department of Physics, Aichi University of Education, Kariya, 448–8542, Japan*

(Received 5 December 2011; accepted 1 March 2012; published online 6 April 2012)

This paper presents an experimental method to predict the operating point of a looped tube thermoacoustic engine combined with an acoustic load. The thermoacoustic engine is divided into two subsystems, one containing the loop and the other containing the load. Their respective acoustic impedances are individually measured using an acoustic driver. Results show that the operating temperature difference and frequency of the loaded engine can be obtained from the measured impedances, before actually combining the subsystems. Furthermore, through measurements of the acoustic power distribution, the frequency best suited to extract the acoustic power from the engine subsystem is identified. Analyzing the subsystems offers a useful method to build a thermoacoustic engine with the desired performance. © *2012 American Institute of Physics*. [http://dx.doi.org/10.1063/1.3700244]

I. INTRODUCTION

A thermoacoustic engine is an acoustical device that utilizes the spontaneous oscillation of a gas column subjected to a steep temperature gradient. The engine is capable of producing intense acoustic waves from heat through good thermal contact between an oscillating gas and the channel walls in a *regenerator*.[1] Critical characteristics of the engine, such as the operating temperature difference and the thermal efficiency, are dependent not only on the regenerator's channel size but also on the combination of tubes that constitute the engine. In 1999, Backhaus and Swift[2] developed a traveling wave engine using a carefully shaped looped tube and a resonator, and reported that the thermal efficiency, the ratio of the output acoustic power to the supplied heat power, reached 0.3 when a temperature difference of 710 K was provided. This efficiency is as high as that of internal combustion engines, in spite of the operation with no moving parts. The extremely simple structure makes it different from conventional heat engines that have mechanical moving parts and sliding seals. Thus, the thermoacoustic engine is potentially a highly reliable, efficient heat engine that can be used for electric generation in satellites[3] and the liquefaction of natural gas.[4]

Although the absence of moving parts is the greatest advantage of thermoacoustic engines, we often encounter a problem intrinsically associated with this advantage. This is the lack of a method (such as the intake and exhaust valves in internal combustion engines) for adjusting the engine performance. For this reason, once the temperature difference goes beyond a critical point, the acoustic variables responsible for thermoacoustic energy conversion are determined automatically according to the engine's design.[5] As a result, we need to repeatedly construct and deconstruct the engine using different tubing and gases, until the desired performance is achieved. Computer simulation[6] is therefore important for testing many engine designs in a short time, while systematic experiments are still necessary to verify the validity of the calculation results. The objective of this study is to propose and examine a method to solve the problem inherent in the thermoacoustic engine.

In this study, we aim to design and build the loaded thermoacoustic engine shown in Fig. 1(a), which consists of a looped tube engine containing a differentially heated regenerator, a load unit made of dynamic bellows closed by a solid plate, and a short branch tube connecting the engine and the load. We begin by separating the engine into two subsystems, A and B, at point O, which is arbitrarily taken on the central axis of the branch tube; subsystem A consists of the looped tube engine and the upper half of the branch tube, and subsystem B consists of the load unit and the rest of the branch tube.

We first focus on the acoustic impedance Z, which is given as

$$Z = \frac{|p|}{A|v|} e^{i\Phi} \tag{1}$$

using the acoustic pressure $P = \mathrm{Re}[pe^{i\omega t}]$, the cross sectional axial acoustic velocity $V = \mathrm{Re}[ve^{i\omega t}]$, and the cross sectional area A; ω is the angular frequency and Φ is the phase by which p leads v. Here Z in subsystem A refers to the acoustic impedance observed at point O, when a gas column is externally driven by the loudspeaker shown in Fig. 1(b), whereas Z in subsystem B is the impedance observed at point O in Fig. 1(c). If the thermoacoustic engine in Fig. 1(a) is to operate spontaneously, the values of Z of subsystems A and B must be identical because of the continuity of pressure and volume velocity at point O. Therefore, measurement of Z should tell us the necessary conditions for spontaneous oscillation to occur, before the subsystems are combined. Second, we measure the acoustic power distribution in subsystem A to analyze the engine performance. The acoustic power is given by

$$I = \frac{A}{2} (\mathrm{Re}Z) |v|^2, \tag{2}$$

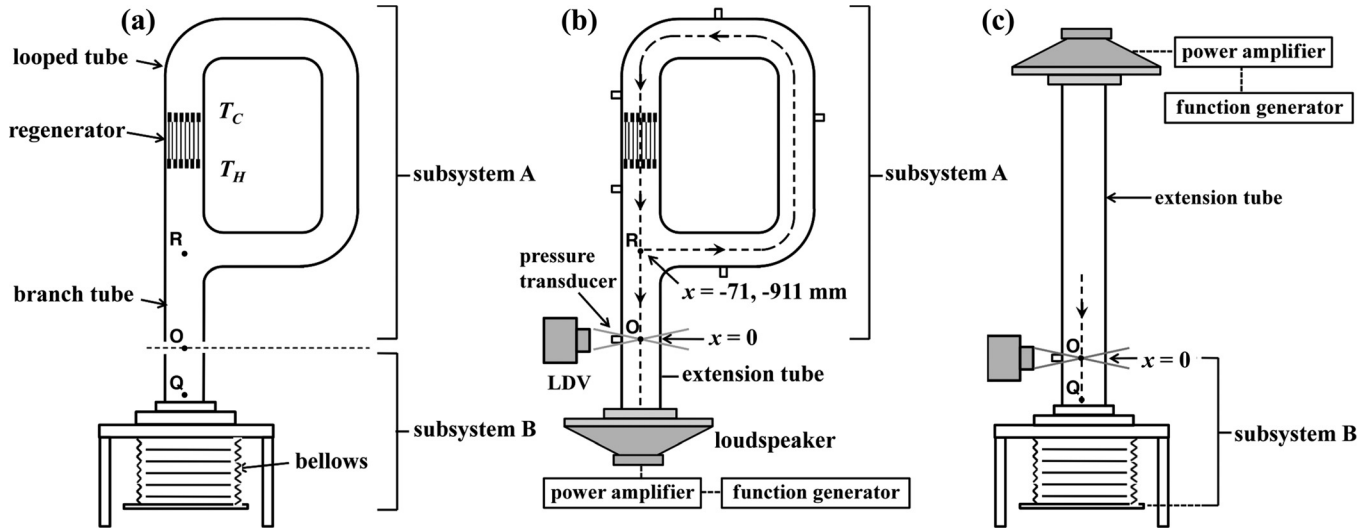

FIG. 1. (a) Loaded thermoacoustic engine, (b) experimental setup for analyzing subsystem A, and (c) that for subsystem B. The origin of the coordinates is taken at point O. The arrows denote the x direction. Point R is at the junction between the looped tube and the branch tube as shown in (a) and (b). Point Q is just above the top flange of the dynamic bellows as in (a) and (c). The lengths RO in (b) and OQ in (c) are the same as those in (a), respectively.

which is also measured using the experimental setup in Fig. 1(b). Use of the acoustic driver enables tests to be done varying either f or ΔT individually. Based on these experimental results, we present a method for designing the loaded thermoacoustic engine.

II. EXPERIMENTS

A. Experimental setup

Figure 1(b) shows subsystem A, the acoustic driver and the extension tube to connect them. Subsystem A is made of a looped tube and a branch tube. The average length of the looped tube is 840 mm, and the length OR of the branch tube is 71 mm. These tubes have identical inner radii of 10.5 mm and are made of transparent acrylic for velocity measurements by a laser Doppler velocimeter (LDV).

The looped tube contains a regenerator, and hot and cold heat exchangers. The 20-mm long regenerator is a stack of 60-mesh stainless-steel screens with a hydraulic diameter of 0.49 mm. The heat exchangers are made of brass plates (0.5 mm in thickness and 10 mm in axial length) aligned parallel with 1 mm spacing. Small copper ducts with inner diameters of 2 mm and lengths of 10 mm are mounted on the tube walls through which we measured the acoustic pressure P with small pressure transducers. Copper tubes are also used for feeding seeding particles (cigarette smoke) into the experimental setup for the LDV measurements. The extension tube has a diameter of 10.5 mm and a length of 39 mm. Its length is arbitrary because it does not affect the Z of the subsystem. A loudspeaker is used as the acoustic driver.

Figure 1(c) shows subsystem B, the acoustic driver, and the extension tube. Subsystem B comprises a branch tube with length OQ = 62 mm and a dynamic bellows closed by a solid plate. The effective diameter and average length of the bellows are 106 and 60 mm, respectively. The extension tube, made of transparent acrylic tube with 10.5 mm inner radius, is 168 mm in length. A small copper duct is mounted on the tube wall at point O for measuring the acoustic pressure at this point.

B. Measurement method

In subsystems A and B, a working gas of air with a mean pressure $P_m = 0.1$ MPa was forced to oscillate by the acoustic driver. The frequency f and the acoustic amplitude were controlled using a function generator and a power amplifier. In subsystem A, the hot heat exchanger temperature T_H was adjusted by an electric heater, whereas the cold heat exchanger temperature T_C was maintained at room temperature 293 K by cooling water. Although an acoustic pressure amplitude $|p|$ of as much as 10% of P_m can be achieved[2] in thermoacoustic engines at a sufficiently high temperature difference $\Delta T = T_H - T_C$, $|p|/P_m$ was kept to below 1% in this experiment. More specifically, $|p|$ at point O in subsystems A and B was maintained at 0.70 kPa throughout the measurements, regardless of f or ΔT.

We simultaneously measured the acoustic pressure P and the axial acoustic particle velocity at point O on the central axis of the tube in subsystems A and B. The cross sectional mean velocity V was obtained from the measured central velocity based on an analytical result from laminar flow theory. (For more details, see Ref. 7.)

III. RESULTS AND DISCUSSION

A. Operating temperature difference and frequency

Figure 2 displays the measured Z of the subsystems in three-dimensional space constructed from a complex plane and a frequency axis. Since the impedance Z of subsystem A gradually changes with the temperature difference ΔT, it is shown as a surface, whereas the values of Z of subsystem B lie on a curve. We confirmed that the curve passes through the Z surface of subsystem A, which will be discussed later.

The projection of the surface onto the complex plane is shown in Fig. 3, where the points for Z of subsystem A with

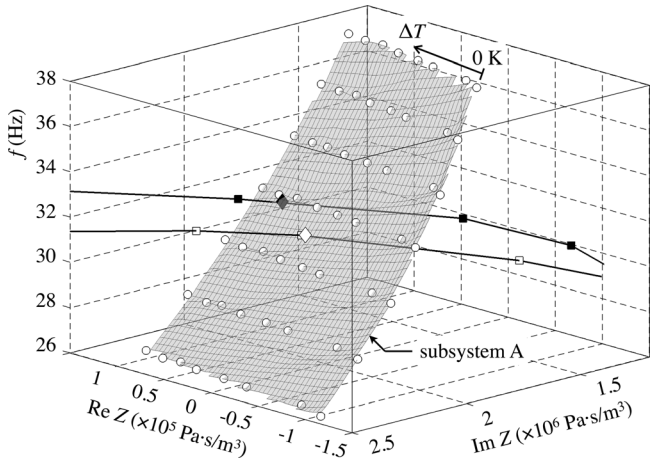

FIG. 2. Complex acoustic impedance Z plotted in three-dimensional space constructed from the complex plane and the frequency-axis. Open circles (○) represent the Z of subsystem A, open (□) and solid squares (■) represent the Z of subsystem B and that of the modified one respectively. Open (◊) and solid diamonds (◆) represent the Z of the combined systems.

equal ΔT and f are each connected by solid and dotted lines, respectively. The real part of Z, Re Z, of subsystem A is consistently negative when $\Delta T \leq 109$ K, but becomes positive with $\Delta T \geq 156$ K. Because Re Z is related to I through $I = \mathrm{A}(\mathrm{Re}\ Z)v^2/2$ as shown in Eq. (2), the sign of Re Z represents whether the flow direction of I is in the positive or negative x direction. Therefore, when $\Delta T \leq 109$ K, the subsystem A acts as an *acoustic energy sink* because I goes in the negative x direction, that is, from the driver to subsystem A. On the other hand, subsystem A starts to function as an *acoustic energy source* when $\Delta T \geq 156$ K, since I flows from subsystem A in the positive x direction. Hence a threshold temperature difference for subsystem A exists, although this depends on the choice of point O. In contrast, since subsystem B is an acoustic load serving as an energy sink, Re Z is always positive. As a result, these two subsystems have an intersection point in the Re $Z > 0$ region at approximately $\Delta T = 300$ K and $30 < f < 32$ Hz. Hence, if these subsystems are connected together, the combined system would operate with the ΔT and f obtained above.

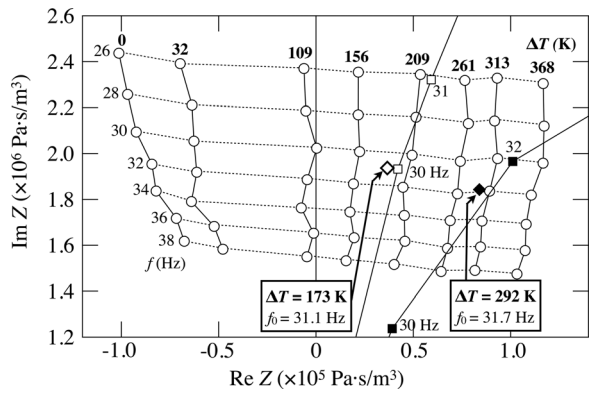

FIG. 3. Acoustic impedance Z of subsystem A (○), subsystem B (■) and the loaded thermoacoustic engine (◆) shown in the complex plane. The Z of the modified subsystem B (□) and that of the corresponding engine (◊) are also shown.

To verify the operation of the combined system, we joined the subsystems and built the loaded thermoacoustic engine shown in Fig. 1(a). When ΔT was increased to 260 K, the loaded thermoacoustic engine started to oscillate spontaneously. When ΔT was further increased to 292 K, the pressure amplitude at point O reached $|p| = 0.7$ kPa, and the frequency f_0 of self-sustained oscillations was 31.7 Hz, as expected from the impedance measurements. The acoustic impedance was measured at point O for the spontaneous oscillation in the loaded thermoacoustic engine. As represented by black diamonds in Fig. 2 and Fig. 3, the Z of the engine agrees well with the intersection point of Z between the subsystems. This result shows that it is possible to predict the operation by judging whether the impedances of the subsystems intersect or not. If they do not intersect, the loaded thermoacoustic engine would not operate. On the other hand, if they do intersect, the loaded thermoacoustic engine would operate with the values of ΔT and f at the intersection point of Z of the two subsystems.

On the basis of this experimental result, we tried to decrease the value of ΔT of the thermoacoustic engine. We modified subsystem B by replacing the dynamic bellows with one having an effective diameter of 62 mm and a length of 52 mm. It was found that the corresponding impedance Z had an intersection point at a lower ΔT, as shown by the white squares in Figs. 2 and 3. In fact, the thermoacoustic engine loaded with the modified subsystem B successfully operated at a lower temperature difference of $\Delta T = 173$ K and $f_0 = 31.1$ Hz. We further tested subsystem B made with a 0.8-meter-long open-ended resonator, instead of the bellows unit. When subsystem A was connected to this resonator, the engine was observed to operate at the ΔT and f determined from the impedance measurements. These results demonstrate the universal applicability of this method to predict the operating point of a loaded thermoacoustic engine.

Many thermoacoustic engines can be thought of as combined systems consisting of fundamental components such as a *resonator*[8] and a *looped tube*.[9] For example, a thermoacoustic electric generator[3] is made of a looped tube, an alternator unit, and a connecting tube; a heat-driven cooler[10] is constructed from two looped tubes and a branch resonator to connect them. Analysis based on the impedance of the subsystems should be useful in finding a combination that realizes the desired operating temperature difference and frequency.

B. Engine characteristics

We have seen that the operating temperature difference ΔT and frequency f_0 of a loaded thermoacoustic engine can be adjusted by exchanging subsystem B with one having a different acoustic impedance Z. The next step is to decide the operating conditions of ΔT and f_0, although the choice of ΔT would be restricted from a practical point of view depending on the temperature of the available heat source. We show here how to find the best frequency that maximizes the output acoustic power of subsystem A at a given ΔT, through measurements of the acoustic power I in subsystem A shown in Fig. 1(b).

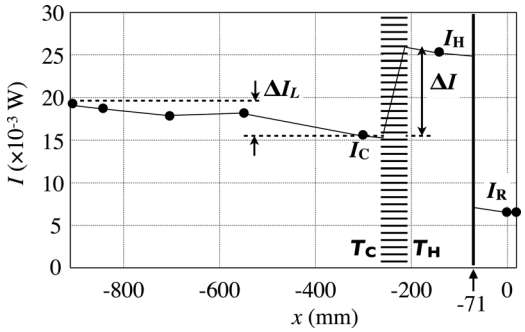

FIG. 4. Axial distribution of I when $f = 40$ Hz and $\Delta T = 308$ K. The region with horizontal lines ($-251 \le x \le -211$ mm) represents the regenerator. The region $-911 \le x \le -71$ mm corresponds to the looped tube; the region greater than -71 mm is the branch duct.

Figure 4 shows the axial distribution of the acoustic power I in subsystem A when $\Delta T = 308$ K and $f = 40$ Hz. The sign of I is always positive. This indicates that I flows counterclockwise in the looped tube and downward in the branch. In the region of the regenerator, an increase in I is observed as it goes from the cold to the hot side. The difference $\Delta I = 9.8 \times 10^{-3}$ W between the acoustic powers I_H and I_C at the sides of the regenerator represents the thermoacoustic power production. Under ideal conditions, where isothermally reversible heat exchange between the gas and solids in the regenerator occurs with negligibly small viscous losses, the acoustic power gain

$$G = \frac{I_H}{I_C} \tag{3}$$

should reach the temperature ratio T_H/T_C.[11,12] The gain G was found to be 1.6, corresponding to 78% of T_H/T_C. On the other hand, I decreases monotonically outside the regenerator. The negative slope dI/dx represents the power dissipation per unit length due to viscous and thermal attenuation at the wall surface. The total decrease ΔI_L in the looped tube amounts to 3.3×10^{-3} W. As a result, the acoustic power that can be used to source subsystem B becomes $I_R = \Delta I - \Delta I_L$ ($= 6.5 \times 10^{-3}$ W), which is seen in the region with $x > -71$ mm in Fig. 4.

From the above observations, we can see that subsystem A should possess a high power gain G in the regenerator and a small power dissipation outside of it, of which the latter can be measured by the ratio

$$\varepsilon \equiv \frac{I_R}{\Delta I}. \tag{4}$$

The ratio ε ranges from 0 to 1, where $\varepsilon = 0$ means that the power produced ΔI is consumed in the looped tube, and $\varepsilon = 1$ indicates that ΔI is delivered to the branch tube without being reduced by energy dissipation in the looped tube.

We determined G and ε through acoustic power measurements with $\Delta T = 0$ and 308 K, and with f from 15 to 85 Hz. The pressure amplitude was adjusted to 0.7 kPa at point O shown in Fig. 1(b). The experimental G is displayed as a function of frequency f in Fig. 5. The horizontal line at $G = 1$ is the dividing line between amplification ($G > 1$) and

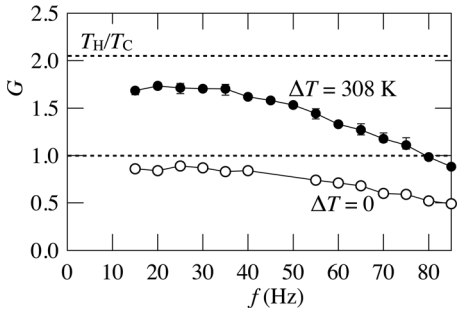

FIG. 5. Acoustic power gain G as a function of frequency f for the subsystem A shown in Fig. 1(b). Open and solid circles represent the data obtained with $\Delta T = 0$ and 308 K, respectively. The dashed lines are drawn at $G = 1$ and $G = T_H/T_C$.

damping ($G < 1$) of the acoustic power, and $G = T_H/T_C$ ($= 2.1$) represents the ideal gain. The gain G with $\Delta T = 0$ decreases with increasing f. This is because the viscous loss increases with f in the regenerator. The difference between G with $\Delta T = 308$ K and that with $\Delta T = 0$ represents the result of thermoacoustic energy conversion in the regenerator. The decrease in gain difference at higher f is attributable to the fact that the higher frequency makes the heat exchange between the gas and the regenerator less perfect. On the other hand, in the frequency region $f < 35$ Hz, G with $\Delta T = 308$ K can retain 85% of T_H/T_C because the heat exchange process is closer to the isothermal one.

Figure 6 shows the ratio ε as a function of f. A broad maximum is observed in the neighborhood of $f = 50$ Hz. From the experimental power gain G and ε shown in Figs. 5 and 6, we consider the best frequency to make both G and ε as large as possible falls into the region from 30 to 40 Hz. Therefore, the subsystem B that has an intersection point in this frequency range should be selected as the counterpart of the present subsystem A. The subsystems B that we used in the preceding section had the desirable impedances because the intersection points were observed at $f = 31.1$ and 31.7 Hz, respectively.

Although G and ε are employed as measures of subsystem A in this study, the thermal efficiency η is of more importance for the practical application of thermoacoustic engines; η is given by

$$\eta \equiv \frac{I_R}{Q_H} = \frac{I_R}{\Delta I} \times \frac{\Delta I}{Q_H}, \tag{5}$$

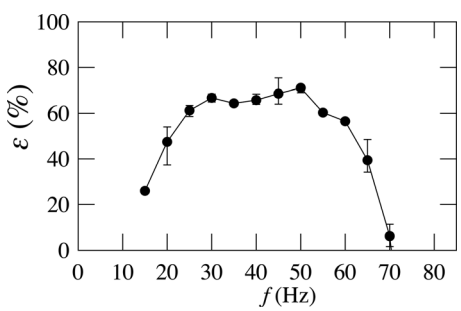

FIG. 6. The ratio ε as a function of frequency f for the subsystem A shown in Fig. 1(b).

where Q_H is the heat supplied to subsystem A necessary to maintain the hot end temperature T_{H}. Here, $\Delta I/Q_H$ is the conversion ratio of the input heat power to the output acoustic power. In other words, $\Delta I/Q_H$ serves as the intrinsic efficiency of thermoacoustic energy conversion in the regenerator. As shown in Eq. (5), $\Delta I/Q_H$ is necessary instead of G for evaluating and analyzing the efficiency. In the future, we will use $\Delta I/Q_H$ and ε to design and build loaded thermoacoustic engines.

IV. SUMMARY

We have presented a method to predict the operating point of a loaded thermoacoustic engine experimentally through measurements of the acoustic impedance of the subsystems. On the basis of this result, we precisely predicted the operating point of the combined thermoacoustic engine before assembling it. Furthermore, through measurements of the acoustic power I in the looped tube, we found the best frequency range of subsystem A to be between 30 and 40 Hz. This fact can be used to choose the appropriate subsystem B. Thus, the analysis of the subsystems offers a useful method for designing thermoacoustic engines experimentally.

[1]G. W. Swift, J. Acoust. Soc. Am. **84**, 1145 (1988) G. W. Swift, *Thermoacoustics: A Unifying Perspective for Some Engines and Refrigerators* (Acoustical Society of America, Sewickley, PA, 2002).
[2]S. N. Backhaus and G. W. Swift, "A thermoacoustic-Stirling heat engine," Nature **399**, 335–338 (1999).
[3]S. Backhaus, E. Tward, and M. Petach, "Traveling-wave thermoacoustic electric generator," Appl. Phys. Lett. **85**, 1085–1087 (2004).
[4]G. W. Swift and J. J. Wollan, "Thermoacoustics for Liquefaction of Natural Gas," GasTIPS **8**, 21 (2002).
[5]Y. Ueda," Thermodynamic cycles executed in a looped-tube thermoacoustic engine", J. Acoust. Soc. Am. **129**, 132–137 (2005).
[6]See http://www.lanl.gov/projects/thermoacoustics/DeltaEC.html for more information about the program DeltaEC.
[7]T. Biwa, Y. Ueda, H. Nomura, and U. Mizutani, and T. Yazaki, "Measurement of the Q value of an acoustic resonator," Phys. Rev. E **72**, 026601 (2005).
[8]T. Yazaki and A. Tominaga, "Measurement of sound generation in thermoacoustic oscillations," Proc. R. Soc. London, Ser. A **454**, 2113 (1998).
[9]T. Yazaki, A. Iwata, T. Maekawa, and A. Tominaga, "Traveling wave thermoacoustic engine in a looped tube," Phys. Rev. Lett. **81**, 3128–3131 (1998).
[10]M. Miwa, T. Sumi, T. Biwa, Y. Ueda, T. Yazaki, "Measurement of acoustic output power in a traveling wave engine," Ultrasonics **44**, 1527–1529 (2006).
[11]P. C. Ceperley, "A pistonless Stirling engine—The traveling wave heat engine," J. Acoust. Soc. Am. **66**, 1508–1513 (1979).
[12]T. Biwa and R. Komatsu, "Acoustical power amplification and damping by temperature gradients," J. Acoust. Soc. Am. **129**, 132–137 (2011).